A High Resolution Bi-atrial Optical Mapping System for the Analysis of Arrhythmia in the Hypertensive Heart

Girish S Ramlugun, Gregory B Sands, Jichao Zhao, Ian J LeGrice, Bruce H Smaill

University of Auckland, Auckland, New Zealand

Abstract

High resolution optical mapping of cardiac activation spread is a powerful tool for investigating the mechanisms of arrhythmia. However, due to the complex geometry of the atria, mapping global electrical activity is challenging. In this study, we present a high resolution optical mapping set-up and a data processing pipeline for characterising bi-atrial arrhythmia. Our system enables recording of bi-atrial electrical activity with high spatial and temporal resolution and provides a flexible tool for programming pacing protocols. Preliminary results indicate that this imaging system and data processing pipeline provide a reliable platform for experimental characterisation of bi-atrial arrhythmia.

1. Introduction

The mechanisms which underlie the initiation and maintenance of atrial fibrillation (AF) are not completely understood [1]. Atrial structural remodelling is strongly associated with AF [2]. It is argued that the texture of fibrosis (interstitial, patchy and diffuse), a consequence of structural remodelling, plays an important role in determining the vulnerability to arrhythmia[3]. The spontaneously hypertensive rat (SHR) replicates key features of human hypertensive heart disease[4]. AF is also inducible in SHR and is associated with atrial structural remodelling [5, 6]. Therefore, SHR provides an appropriate animal model for investigating atrial arrhythmogenicity.

Optical mapping is a powerful tool for recording activation spread and modern cameras enable the acquisition of electrophysiological data with high spatial and temporal resolution. However, due to their complex geometry and limited size, optical mapping of the murine atria has either been restricted to small regions[7] or the atria have been dissected and flattened[8, 9]. While the latter approach offers a better view of the global activity, dissection can alter the structural integrity of atrial tissue and influence functional behaviour. The goal of this work is to determine the feasibility and reliability of an anatomically intact, isolated murine atrial preparation for investigating mechanisms of atrial arrhythmia.

2. Materials and methods

2.1. Atrial Preparation

All surgical procedures were approved by the Animal Ethics Committee of the University of Auckland and conform to the Guide for the Care and Use of Laboratory Animals (NIH publication no. 85-23). Experiments were conducted using age-matched female SHRs at 6/7 months, (n=6), 12/13 months (n=8), and 18 months, (n=6). Animals were anaesthetised with isoflurane and euthanized by cervical dislocation. After thoracotomy, heparin ($\sim$100 U/kg) was injected into the left ventricle and allowed to circulate for 30s. The heart was rapidly excised, mounted on a Langendorff apparatus and perfused with Krebs-Henseleit buffer (KHB) containing (in mM): 118.0 NaCl, 4.7 KCl, 1.2 KH_2PO_4, 1.2 $MgSO_4$, 1.8 $CaCl_2$, 25.0 $NaHCO_3$, and 11.1 glucose bubbled with 95% O_2-5% CO_2. The heart was immersed in the oxygenated KHB and excess fat and connective tissue were dissected from the surface. The atria were then isolated by transection at the atrioventricular annulus.

Custom-made silver wire pacing electrodes were inserted into both atrial appendages using a 27.5 gauge needle introducer. The atria were then pinned down in a superfusion chamber containing Ag-AgCl recording electrodes (Figure 1) and a temperature sensor. Oxygenated KHB was circulated through the chamber temperature was maintained at 37$\pm$1°C. Following development of stable sinus rhythm (SR), superfusion was interrupted and the atria were stained with 10 μM di-4-ANEPPS (Biotium, CA, USA) in oxygenated KHB for 10 minutes. Superfusion was then resumed and a bolus of the mechanical uncoupler, blebbistatin (final concentration of 5 μM), was added to the perfusate. In most cases, the preparation was stable (sustained SR) for at least 3 hours, during which the recordings were taken. Dye and uncoupler reloading were not subsequently required.

 ISSN: 2325-887X DOI:10.22489/CinC.2017.108-431

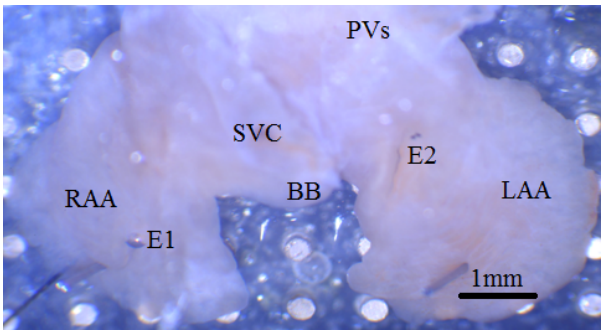

Figure 1. Photograph of a typical preparation in the recording chamber. Legend: RAA, right atrial appendage; E1 & E2, pacing electrodes; SVC, superior vena cava; BB, Bachmanns bundle; LAA, left atrial appendage

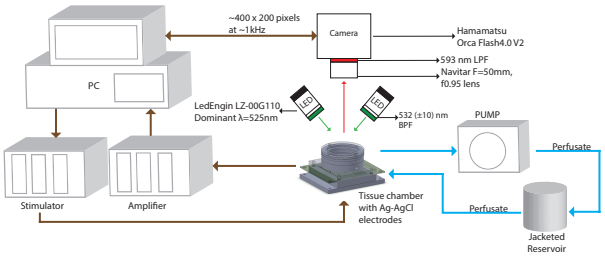

Figure 2. Schematic of the experimental set-up

2.2. Data Acquisition

Optical action potentials were recorded from the epicardial surface through a glass window. Excitation light was provided by two 10 W LEDs (LedEngin LZ4- 00G110), each fitted with an aspheric condenser lens for collimation and a 532 nm laser line band-pass filter (Thorlabs Inc, NJ, USA). The LEDs were battery-powered and a custom circuit was built to control intensity and switching. Emitted light was filtered with a 593 nm edge long-pass filter (Semrock Inc, NY, USA). Images were acquired with a high speed scientific CMOS camera (Orca Flash 4.0 v2, Hamamatsu, Japan) at $\sim$1000 frames per second. The camera was fitted with a fast lens (Navitar DO-5095, 50 mm, F/0.95) on a 5mm spacer. The effective field of view was $\sim$400x200 pixels at $\sim$26 μm per pixel.

A global atrial electrogram was recorded between two Ag-AgCl electrodes in right and left atria using an AC-coupled differential amplifier (LP122, Grass Technologies, Ireland). This signal was digitised with an NI PCI-6255 acquisition board (National Instruments, TX, USA) and acquired at 100 kHz. Atrial pacing was carried out with a purpose-built constant-current stimulator driven by an external pulse train. The stimulator consisted of a LT3092 (Linear Technology, CA, USA) programmable current source with MOSFET switching. Output current was set by a microcontroller (Arduino Mega, Arduino AG, Italy).

A custom user interface written in the LabVIEW (National Instruments, Austin, TX) programming language was used to 1) specify stimulus parameters and sequences, 2) drive the stimulator, 3) switch LEDs, 4) control the camera and 5) acquire bath temperature, global electrogram, camera trigger signal and image frames. The system could be used interactively for experiment set-up and in programmed mode for recording electrical responses to specified pacing sequences. Finally, the interface offered a wide range of data processing and visualisation options.

2.3. Experimental Protocol

Optical and electrical recordings were acquired during programmed stimulus sequences and in SR before and after each stimulus sequence. The threshold current for stable pacing was determined for each pacing site and 2x threshold current was used throughout. Restitution kinetics were characterised by imposing sequences of 10 S1 pulses across cycle lengths in the range (100-350) ms. Arrhythmia susceptibility was tested with an S1-S2 protocol [6]. S1-S1 interval was set at 250ms and S1-S2 was decremented until capture was lost or an arrhythmia was initiated. Stimulation was terminated with the onset of arrhythmia. All pacing protocols were repeated for right and left atria. Saved recordings were processed on the fly to provide feedback throughout the experiment. After the experiment, an image of the preparation was acquired together with a linear scale to calibrate pixel dimensions.

2.4. Data Processing and Analysis

The camera trigger signal was used to align electrical and the optical recordings (Figure 3). In regular rhythms (i.e stable SR or S1 pacing), the electrogram was used to ensemble-average optical signals and improve signal-to-noise ratio(SNR). A mask was created interactively for each image to segment the atrial boundary and was subdivided into right and left atria. Further processing involved the following:

1. 2x2 binning of images.
2. Spatial filtering with a Gaussian kernel to improve SNR.
3. Wavelet denoising in the temporal domain. The discrete wavelet transform was computed using Daubechies wavelet db06. Thresholding was performed using Stein's unbiased risk estimate (SURE) algorithm.
4. Removal of background fluorescence(F) and signal inversion at each pixel by subtracting median.
5. Temporal smoothing using Savitsky-Golay filters.

Each experiment resulted in a series of recordings representing the functional properties of the atria under different

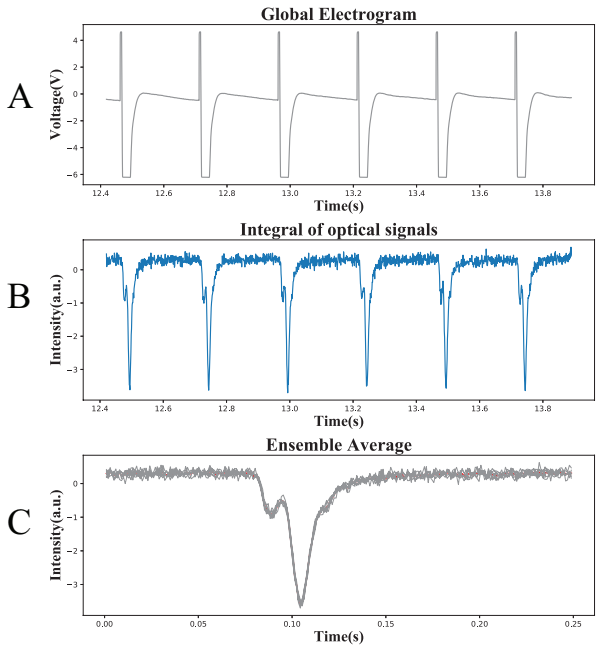

Figure 3. Ensemble averaging of paced signals (250ms cycle length). A: Global electrogram, B: Integral of optical signals, C: Integral of ensemble averaged optical signals.

conditions (e.g., SR, pacing, arrhythmia). Each recording was saved as a separate file, which was then entered in a SQLite relational database. This enabled the data to be clustered and queried from the database by defining a set of parameters to be analysed (such as age, pacing interval, pacing site, APD distribution etc.). Python scripts were written to query and analyse data and for plotting results.

Activation maps were generated by calculating the activation time (AT) for each pixel. AT was defined as the maximum change in fluorescence (dF/dtmax) during the action potential upstroke. The derivative of the action potential was calculated by convolving the images with the derivative of a Gaussian function in the temporal domain. Action potential duration (APD80) was calculated for each pixel by finding the duration between the AT and time of 80% repolarisation (the time after the upstroke at which the fluorescence is 20% of the maximum). Because of the APDs in murine atria, the signal was first oversampled to get a better estimate of repolarisation times.

Phase maps were generated for recordings which consisted of sustained re-entry patterns with a phase singularity point located in the field of view. The period of the signal was estimated using the Buneman algorithm[10]. A previously described method for reconstructing instantaneous phase of unipolar contact electrograms [11] was adapted to obtain phase maps.

3. Results and Discussions

Activation patterns observed during SR (Figure 4A) were consistent with previous studies [8]. The site of initial breakthrough in the sinoatrial node (SAN) was variable, alternating between the inferior and superior regions of the crista terminalis (CT). Activation spread uniformly across the RA via the CT and more slowly to the LA (Figure 4A). APD values in the SAN region were consistently higher than in other atrial regions (Figures 4B,C). Despite this, APD distribution was wider in the LA than the RA. Maintenance of constant chamber temperature was necessary to minimize variability in sinus rate and conduction velocity.

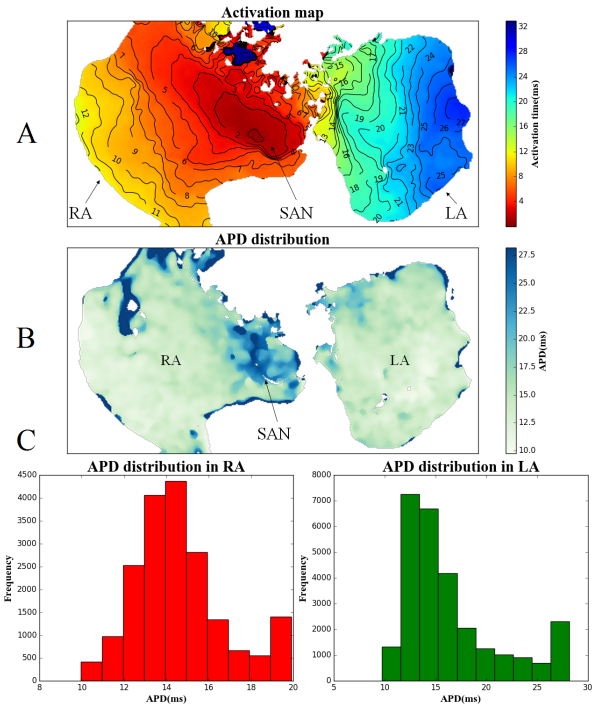

Figure 4. Representative result: A, Activation map at SR; B, APD distribution; C, Histogram of APD for each atrium.

An important novel feature of our experimental preparation is that maintenance of the structural and functional integrity of the atria, enabled us to observe and analyse numerous instances of macro reentry. Rate-dependent interatrial conduction block was consistently observed in most animals. In cases where sustained arrhythmia was induced, the global electrogram showed patterns of atrial flutter (Figure 5B) and a typical example is illustrated in Figure 5. Regions of interest R1 and R2 were selected to represent global activity in the RA and LA respectively. The integral of the optical signals (Figure 5C) indicate the alternating but rhythmic nature of conduction. Corresponding results

for R1 and R2 (Figure 5D) clearly demonstrate 3:1 conduction block from the RA to LA. Instantaneous phase was estimated (Figure 5E) and this enabled the construction of phase maps (Figure 5F). The study in Figure 5 illustrates a rhythmic activation pattern with a cycle length of 47 ms, in the RA. A stationary phase singularity is located in the centre of the RAA.

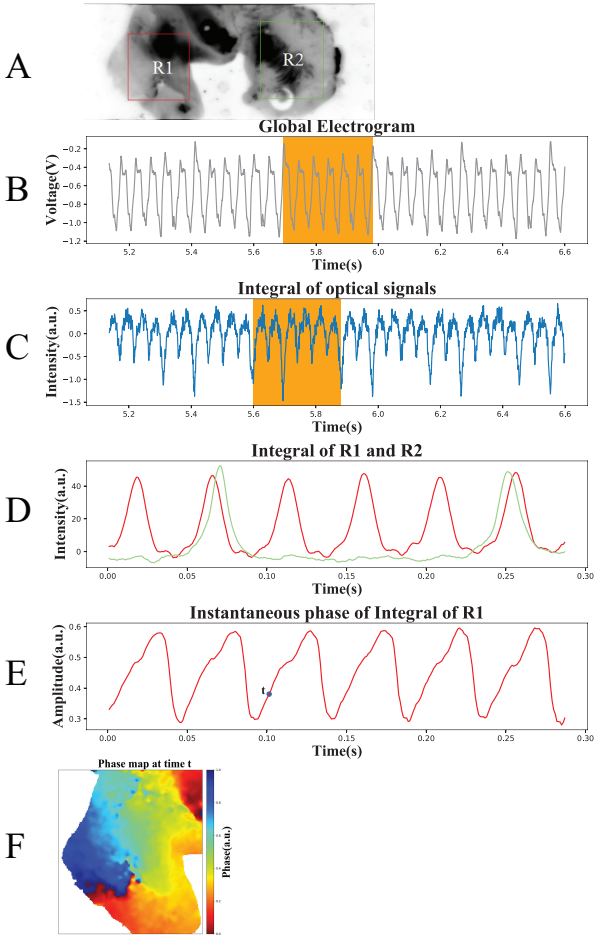

Figure 5. A, Grayscale image defining ROIs in each side of the atrium; B, Global electrogram of the arrhythmia; C: Integral of the optical signals; D, Single cycle (highlighted in B,C) of integral of R1(red) and R2(green); E, Instantaneous phase in R1; F, Phase map at time t

4. Conclusions

This work illustrates the unique capabilities of our high resolution optical mapping set-up for characterising global activation spread in the atria. Because the anatomical integrity of the atria is substantially preserved in our preparation, we have been able to demonstrate and analyse macro-reentry. Preliminary studies have been carried out in SHRs. Future work will be directed at systematic time-course studies in this animal model of hypertensive heart disease and expanding our database which links increasing propensity to atrial electrical dysfunction with both structural and electrical remodelling in these animals.

Acknowledgements

This research was supported by the Health Research Council (HRC) of New Zealand. We would also like to thank Linley Nisbet and Greg Dawick for technical support.

References

[1] Andrade, J. et al. The Clinical Profile and Pathophysiology of Atrial Fibrillation: Relationships Among Clinical Features, Epidemiology, and Mechanisms. Circ Res 2014;14(9), 1453-1468.

[2] Kostin, S. et al. Structural correlate of atrial fibrillation in human patients, Cardiovas Res, 2002;54(2):361-79.

[3] de Jong S. et al. Fibrosis and cardiac arrhythmias. J Cardiovasc Pharmacol. 2011 Jun;57(6):630-8.

[4] LeGrice, I. J. et al. H. Progression of myocardial remodeling and mechanical dysfunction in the spontaneously hypertensive rat. Am J Physiol Heart Circ Physiol. 2012;303(11):H1353-65.

[5] Lau, D. H. et al. Atrial Arrhythmia in Ageing Spontaneously Hypertensive Rats. PLoS ONE.2013;8(8).

[6] Parikh, A. et al. Relaxin suppresses atrial fibrillation by reversing fibrosis and myocyte hypertrophy and increasing conduction velocity and sodium current in spontaneously hypertensive rat hearts. Circ Res. 2013;113(3):313-21.

[7] Yu, Y. T. et al. Optical mapping design for murine atrial electrophysiology. Comp methods in Biomechanics & Bio. Engg.2015;1163;1-9

[8] Schmidt, A., Nygren, A. Optical mapping system for visualizing arrhythmias in isolated mouse atria, Proc of IEEE EMBS. 2006,4002-4005.

[9] Glukhov, A. et al. Functional anatomy of the murine sinus node: high-resolution optical mapping of ankyrin-B heterozygous mice. Am J Phys. 2010;29(2);482-491.

[10] Buneman, 0. A compact noniterative poisson solver.1969;SUIPR-294;Stanford University

[11] Kuklik, P. et al. Reconstruction of instantaneous phase of unipolar atrial contact electrogram using a concept of sinusoidal recomposition and hilbert transform. IEEE Trans Bio. Engg. 2015;62(1);296-302

Address for correspondence:

Girish Ramlugun
Auckland Bioengineering Institute
University of Auckland
Auckland, New Zealand
gram526@aucklanduni.ac.nz